Scanning tunneling microscopy of Ag growth on GaAs(110) at 300 K: From clusters to crystallites

B. M. Trafas, Y.-N. Yang, R. L. Siefert, and J. H. Weaver
Department of Materials Science and Chemical Engineering, University of Minnesota, Minneapolis, Minnesota 55455
(Received 14 December 1990)

Scanning-tunneling-microscopy (STM) studies of Ag overlayer growth on GaAs(110) at 300 K show cluster nucleation at low coverage followed by conversion to nanocrystallites with distinct facets. Clusters formed by depositions below ~0.5 monolayer (ML) Ag exhibit no apparent preferential substrate orientation, and individual atoms within the clusters cannot be resolved. These are three-dimensional (3D) clusters, as shown by calculations of cluster volumes and areas based on the STM images, and they contain up to ~250 atoms. Continued deposition yields new small clusters in addition to the growth of existing clusters and the coalescing of clusters in close proximity. By ~5 ML deposition the Ag structures exhibit crystalline order and expose {111} facets. The evolution from clusters to crystallites also involves a preferential orientation so that $[1\bar{1}0]$ of Ag is parallel to $[1\bar{1}0]$ of GaAs(110) and the Ag overlayer (111) plane is tilted 25° around the $[1\bar{1}0]$ direction of GaAs(110). The overlayer derived from these 3D crystallites is then highly irregular, and contact with the partially relaxed GaAs(110) surface is achieved through regularly stepped Ag(110) planes. These results demonstrate weak substrate interaction and cooperative Ag rearrangement to minimize surface energies, even at 300 K.

INTRODUCTION

Issues related to the structure and properties of metal-semiconductor interfaces have attracted interest for many years.[1-4] Three growth modes for nonreactive overlayers have been discussed at length.[4] One involves layer-by-layer growth on the substrate, the second involves the nucleation of three-dimensional (3D) clusters directly on the surface, and the third describes the formation of one monolayer (ML) but then 3D cluster growth on that layer. These growth modes reflect absorbate-absorbate and absorbate-substrate bonding energies. To date, however, it has not been possible to predict the specific growth modes for a given system because the interactions are complex and because kinetic considerations come into play. However, studies using scanning-tunneling microscopy (STM) have provided real-space images of surfaces and evolving interfaces,[5-15] and these images offer critical information about overlayer structure and properties.

Most studies of metal overlayer formation on semiconductor surfaces have involved growth on Si(111), Si(100), GaAs(110), and GaAs(100). For metal-GaAs(110) systems, photoemission investigations[1] have distinguished between overlayers characterized as highly reactive (Ti,Sm), disruptive but weakly reactive (Cr,Fe,Au), and nondisruptive (Ag,Bi,Sb,Sn). STM has now been used to investigate the structural properties of several of these systems.[10-15] They have shown, for example, that clusters form when Cr (Ref. 10) and Fe (Ref. 11) atoms are deposited from a thermal source onto GaAs(110) at 300 K. As growth continues, 3D structures with characteristic dimensions of 45–60 Å are observed, but these aggregates do not exhibit a preferred orientation relative to the substrate. For Cr, the failure to establish an epitaxial-growth pattern has been attributed to substrate disruption and the encorporation of Ga and As atoms within the Cr aggregates [bcc Cr is lattice matched to GaAs(110) to within 1.8%].[10] Cluster formation also occurs at low coverage for Au atom deposition at 300 K onto GaAs(110).[12] These clusters exhibit a distinct epitaxial relationship with the substrate when they grow in size, even though Au deposition also induces limited substrate disruption.[1,16]

This paper focuses on the nucleation and growth of Ag on GaAs(110) at 300 K. This system has been characterized as nondisruptive and photoemission studies have concluded that clusters grow.[1,17] Our STM studies of submonolayer and monolayer coverages show the evolution of isolated 3D clusters as they grow, coalesce, and ultimately assume crystalline form in registry with the substrate. Parallel low-energy electron diffraction (LEED) studies demonstrate that facets observed in STM correspond to {111} surfaces. We propose a model for these growth structures in which the Ag(110) surface matches the partially relaxed GaAs(110) surface, but periodic steps are introduced every four atoms along $[00\bar{1}]$ to maintain registry.

EXPERIMENT

The STM experiments were performed at pressures of $\sim 8\times 10^{-11}$ Torr in an ultrahigh-vacuum chamber optimized for interface research.[13] The microscope, purchased from Park Scientific Instruments,[18] consists of a rigid Al frame with a double spring suspension and magnetic damping for vibration isolation, a linear translation stage and stepper motor for coarse sample motion, and a piezoelectric tripod for tip motion. The STM images were acquired at room temperature in a constant tunneling current mode. The tunneling currents were between 0.1 and 0.5 nA, and the tunneling voltages ranged from 0.8 to 2.5 V. GaAs(110) surfaces were prepared by cleav-

ing $3\times4\times10$ mm^3 posts. Images presented in this paper were acquired with samples that were Zn doped at 3×10^{19} cm^{-3}, but n-type samples doped with Si at 4×10^{18} cm^{-3} were also used for studies of clean surfaces. Tunneling tips were formed by electrochemical etching of polycrystalline tungsten wire. These tips were heated *in situ* using electron bombardment to remove residual tip oxides prior to the measurements.

Silver was evaporated from resistively heated tungsten boats located ~30 cm from the sample surface. During evaporation, the system pressure was below 4×10^{-10} Torr. The evaporation rates were 1 Å per 100–200 s, as determined using a calibrated quartz-crystal microbalance located near the sample. The sample was exposed to the source only after the evaporation rate had been stabilized. For GaAs(110), 1 ML corresponds to 8.85×10^{14} atoms/cm^2. This is equal to the deposition of 1.51 Å of Ag. We express the amount of material deposited in terms of GaAs(110) monolayers, but the results will demonstrate that growth is not layer by layer. Moreover, the planar density for Ag(110) is 96% that of GaAs(110), namely 8.46×10^{14} atoms/cm^2. Images were obtained for depositions of 0.01, 0.05, 0.1, 0.25, 0.5, 1.5, 5, 10, and 20 ML of Ag. LEED studies were done at each coverage after the STM experiments were concluded. Estimates of the volume of the Ag clusters were made by integrating the STM height contours of the clusters.[11]

RESULTS AND DISCUSSION

The GaAs(110) surfaces used for these studies were produced by cleaving relatively large posts. Most cleaves produced regions that were mirrorlike over large fractions of the surface. STM images obtained from these specular surfaces showed atomically flat regions extending hundreds of Ångstroms laterally separated by single-height steps. Images acquired with sample biases of 1.9 and −1.9 V and tunneling currents of 0.1 nA revealed chains that could be distinguished as Ga or As derived with a 1×1 unit cell measuring 4.0×5.64 Å^2, as was shown by Feenstra *et al.*[19] Negative sample voltages highlighted the occupied electronic states (As atoms), while positive voltages reflected the unoccupied states (Ga atoms). The STM images also revealed various types of surface defects that resulted from cleaving. Single vacancies (As defects visible in occupied-state images) and divacancies (Ga-As defects visible in both unoccupied- and occupied-state images) were observed. These can be compared to the results of Whitman *et al.*[20] for InSb(110) where defects related to anion and Schottky vacancies were identified. STM images acquired for many different cleaves showed that the defect density did not correlate with either the dopant type or concentration, and even cleaves from the same post could have different defect densities. We conclude that it is not possible to predict the defect density for a given cleave. At the same time, changes in the number of defects following atom deposition could be observed readily.[10] It is important to note that I-V measurements for p-type samples indicated that the surface Fermi levels were unpinned, even when defect densities exceeded ~10^{12} cm^{-2}, a number thought to be sufficient to pin the surface Fermi level if they were electrically active.[21] In the course of these STM studies,

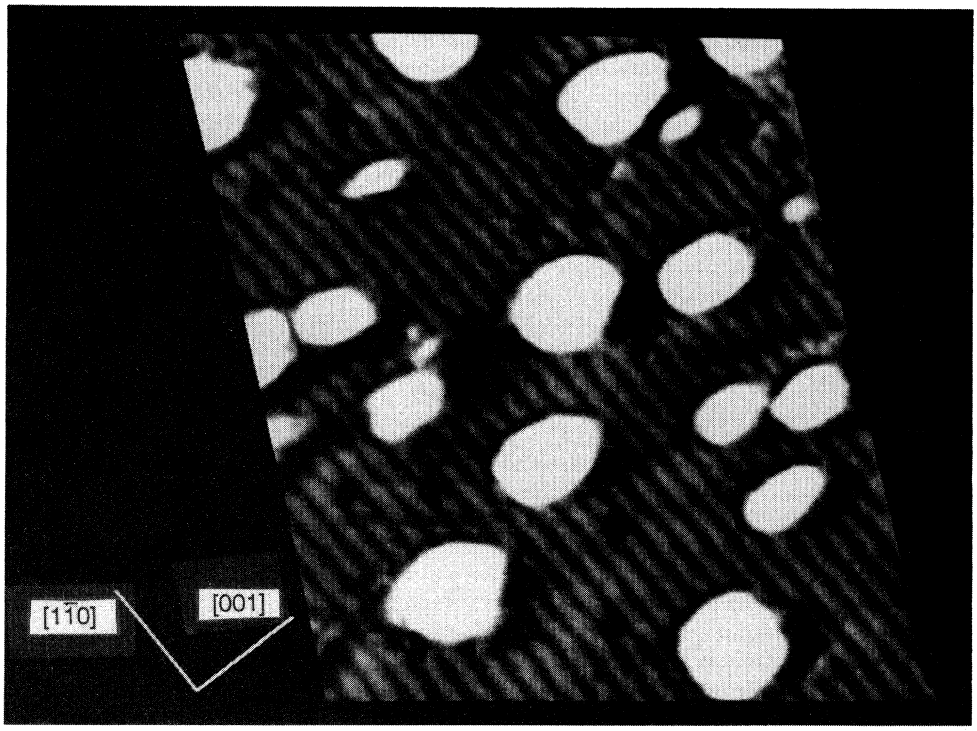

FIG. 1. STM image of GaAs(110) following evaporation of 0.25 ML of Ag at 300 K for an area of 120×120 Å^2. The image was acquired with a sample voltage of −1.9 V and corresponds to imaging As atoms. Dark depressions represent surface defects, whereas the bright areas reflect 3D clusters of Ag. The typical volume of these clusters is ~150–2500 Å^3.

steps of various densities and directions were also observed.[22] For the Ag growth studies discussed here, the surfaces were selected on the basis of the low density of surface defects and steps.

Silver atoms deposition at 300 K led to the formation of clusters on GaAs(110), and these appeared as bright spots in STM images obtained under both positive and negative sample bias. Repetitive scanning across the clusters showed that they were stable and did not change with time. (We have also observed tip-cluster interactions, and they will be discussed later.) A simple integration of the cluster contours verified that the coverage corresponded to the amount of Ag deposited, with nothing that might be related to Ga- or As-derived structures, in agreement with photoemission results that showed nonreactive overlayer growth.[1,17] There was no indication of disruption induced by Ag deposition, judging from the defect density for the clean surface and the Ag-exposed surface. Variations in the imaging conditions led to only slight contrast changes for the Ag clusters ($-2.5 < V_t < 2.5$ V; $0.1 < I_t < 0.5$ nA), and we conclude that the STM images reflect the surface topography under these imaging conditions.

Figure 1 shows an image for GaAs(110) onto which 0.25 ML of Ag had been deposited at 300 K (area $\sim 120 \times 120$ Å^2). This image is representative of the low-coverage regime, 0.01–0.25 ML. The substrate appears as rows of (As) atoms along $[1\bar{1}0]$, as labeled, with drift correction to show the clusters without distortion. In this coverage range, there was no evidence of isolated Ag atoms or ordered Ag structures. Moreover, individual Ag atoms within the clusters were not resolvable. Topographic profiles across the clusters showed that the clusters were three dimensional with volumes ranging from ~ 150 to 2500 Å^3 after 0.25-ML deposition.

Figure 2 shows the evolving Ag overlayer morphology via images obtained after successive depositions to give 0.5, 1.5, 5, and 10 ML of Ag on a single GaAs(110) surface. The images were acquired with a negative sample bias (As atoms). The diagonal lines define the $[1\bar{1}0]$ direction, and the gray scale was computed according to surface illumination from a point in the upper-right corner of the image. This presentation helps to visualize the transition from clusters [Fig. 2(a)] to crystallites [Fig. 2(d)] by enhancing Ag facets as they become apparent.

Figure 2(a) shows Ag clusters after 0.5-ML deposition onto an area of 220×220 Å^2. The average cluster size at this coverage is greater than at 0.25 ML, and some of the clusters have merged. The presence of smaller clusters also indicates that the nucleation density is not constant. Again, there is no obvious preferred orientation with respect to the substrate. The clusters do not appear to be crystalline although the larger clusters may contain ~ 250 atoms, while most contain ~ 150 atoms and are probably metallic.

The Ag morphology on GaAs(110) produced by additional deposition to 1.5 ML is dominated by large clusters, as shown in Fig. 2(b) for a 320×320 Å^2 area, with relatively small clusters in the more open areas. This suggests that the effective diffusion length of a Ag atom condensed at 300 K is larger than the average distance between clusters. Silver deposition would then favor growth for existing clusters rather than the nucleation of new ones at 300 K. Such 3D growth is also enhanced when Ag atoms condense onto existing clusters. Extensive cluster coalescence is evident by 1.5-ML deposition, and topographic shading gives some indication of crystalline faceting. There is no evidence of grain boundaries for large structures formed by coalescence. This suggests that the energy released upon such coalescence may assist in atom rearrangement and the transformation to ordered structures, i.e., kinetic constraints were not severe.

The continued deposition to 5 ML of Ag on GaAs(110) produces a surface that is covered by Ag, as is evident from the image of Fig. 2(c) for an area 425×425 Å^2. At this stage of film growth, there is clear evidence of cluster coalescence and the formation of structures that appear rectangular in plan view. The long axis of these rectangles is parallel to the GaAs $[1\bar{1}0]$ direction and the short axis is along [001]. This demonstrates that a relationship with the substrate has been established that was not evident at lower coverage due to significant atom redistributions. Again, the kinetic constraints on such movement seem to be overcome easily for growth at 300 K. Cross-sectional measurements of these structures show sizes that are consistent with the coalescence of 4–6 of the larger clusters of Fig. 2(b). Even so, a smooth continuous layer has not been formed.

When the amount of Ag deposited onto GaAs(110) is increased to the equivalent of 10 ML, the STM images reveal distinct Ag crystallites, as is evident from Fig. 2(d) for a representative 425×425 Å^2 area. These crystallites rise from regions where the morphology appears more irregular and where the amount of Ag is much smaller. Unfortunately, it is impossible to estimate the thickness of this base layer. One can speculate that the disorder reflects the fact that there are too few Ag atoms to induce a transformation to a more ordered nanocrystallite. (The bottom-right corner appears to be flat, but this is an artifact of clipping by the feedback electronics.) The larger scale morphology is dominated by structures roughly 80–100 Å in length that are elongated along the $[1\bar{1}0]$ direction of the substrate, with well-defined [001] relationships as well with characteristic lengths of 60–70 Å. Distinct facets, steps, and terraces are evident but individual atoms cannot be resolved.

Figure 3 shows mosaic images for 5 and 10-ML Ag deposition. They were derived from individual images covering $\sim 415 \times 425$ Å^2 collected with a sample bias of -0.8 V and a tunneling current of 0.5 nA to enhance the resolution of the overlayer features. The alignment with the substrate $[1\bar{1}0]$ and [001] directions is again apparent with larger dimension along $[1\bar{1}0]$. In principle, such a growth structure could reflect the initial diffusion of Ag on the substrate,[23] but no elongation along $[1\bar{1}0]$ was evident in the images at lower coverage. Hence, the apparent asymmetry of the crystallites is related to the growth of the Ag films rather than the initial diffusion. Facets for the larger structures are clearly evident.

To determine the crystallographic orientation of the Ag facets, we acquired LEED patterns for each coverage after completion of the STM measurements. The sharp

1×1 pattern of the clean surface faded slowly with Ag deposition, persisting to ~1.5-ML deposition but with very low intensity and a high background. Whereas only the substrate pattern was observed for coverages below 0.75 ML, very faint streaks parallel to the substrate [001] direction with a hexagonal symmetry were apparent by ~1.5 ML. These streaks intensified, and a clear hexagonal LEED pattern was observed with deposition to 10 ML. The symmetry and spot separation of such patterns are indicative of diffraction from Ag(111) surfaces. The appearance of a hexagonal LEED pattern with spots extended in the [001] direction demonstrates that the crystallites are shorter in [001] compared to [1$\bar{1}$0], in agreement with the STM images. Our LEED observations agree with those from the more exhaustive LEED investigation of Bolmont *et al.*[24] for Ag growth on GaAs(110). Their analysis indicated that the Ag(111) facets were inclined ~25° from the substrate around the [1$\bar{1}$0] direction, not parallel to the substrate. Confirmation of this conclusion can be obtained from STM cross-sectional scans.

Figure 4(a) shows a closeup STM image of a typical crystallite formed by 10-ML Ag deposition onto GaAs(110) at 300 K to emphasize the different {111} facets. The lines $A-A'$ and $B-B'$ are parallel to the [001] and [1$\bar{1}$0] directions of GaAs(110), respectively, and Fig. 4(b) shows cross-sectional views of the crystallite along these lines. While the shape of the tunneling tip

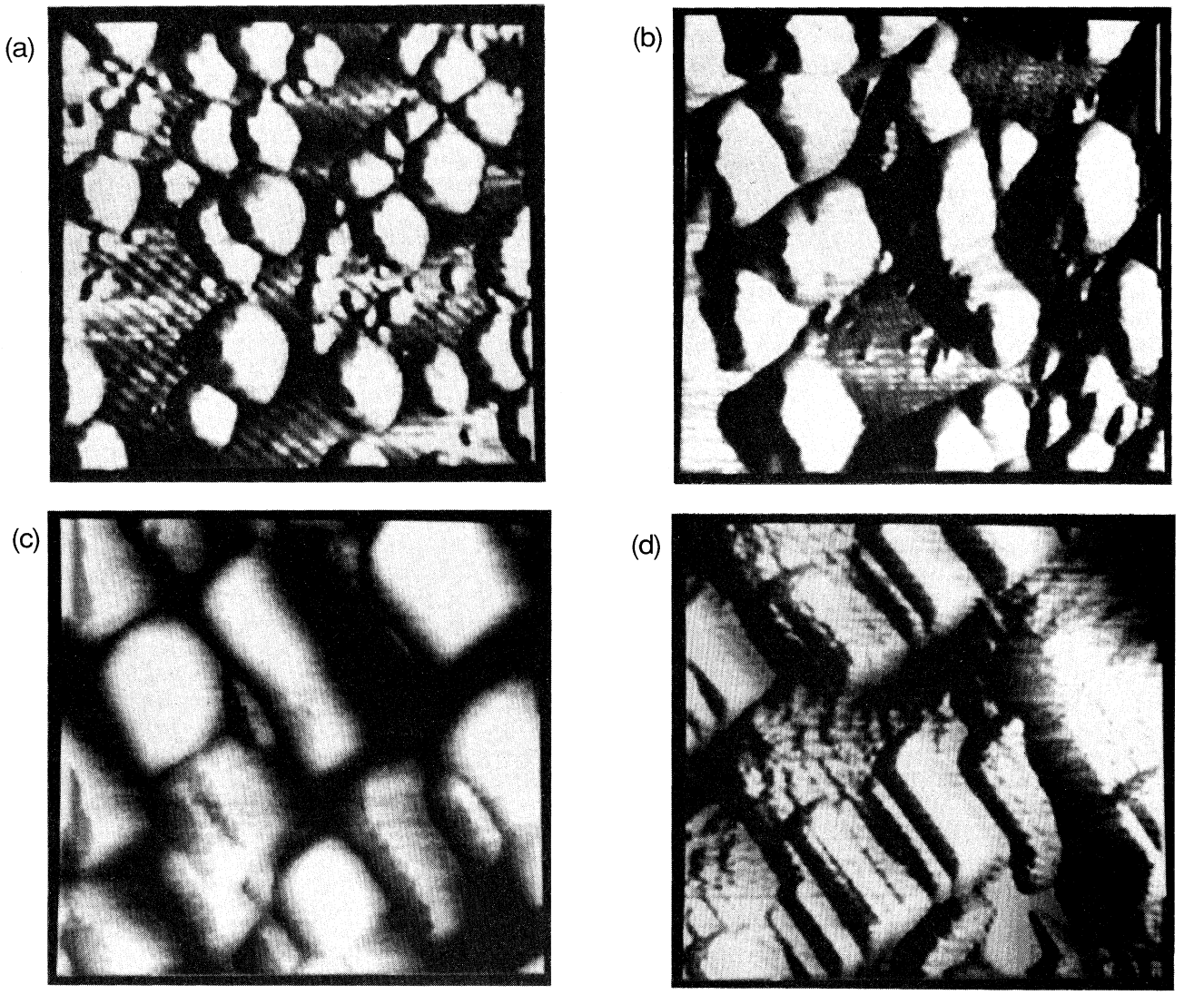

FIG. 2. (a)–(d) STM images of Ag overlayer growth by atom deposition onto GaAs(110) at 300 K for coverages of (a) 0.5, (b) 1.5, (c) 5, and (d) 10 ML of Ag on GaAs(110). The areas imaged are 220×220, 320×320, 425×425, and 425×425 Å^2, respectively. Images (a) and (b) were obtained with a sample bias of −2.5 V and a tunneling current of 0.1 nA. Images (c) and (d) were obtained with −0.8 V and 1 nA to enhance the contrast of the metal surface. The gray scale in these images is computed according to a surface directional derivative, corresponding to illumination from a point in the upper-right corner of each image. Ag clustering is apparent in (a) and (b). Faceting and the transition to crystallites is evident in (c) and (d) where the long dimension is along [1$\bar{1}$0] and the short dimension is along [001].

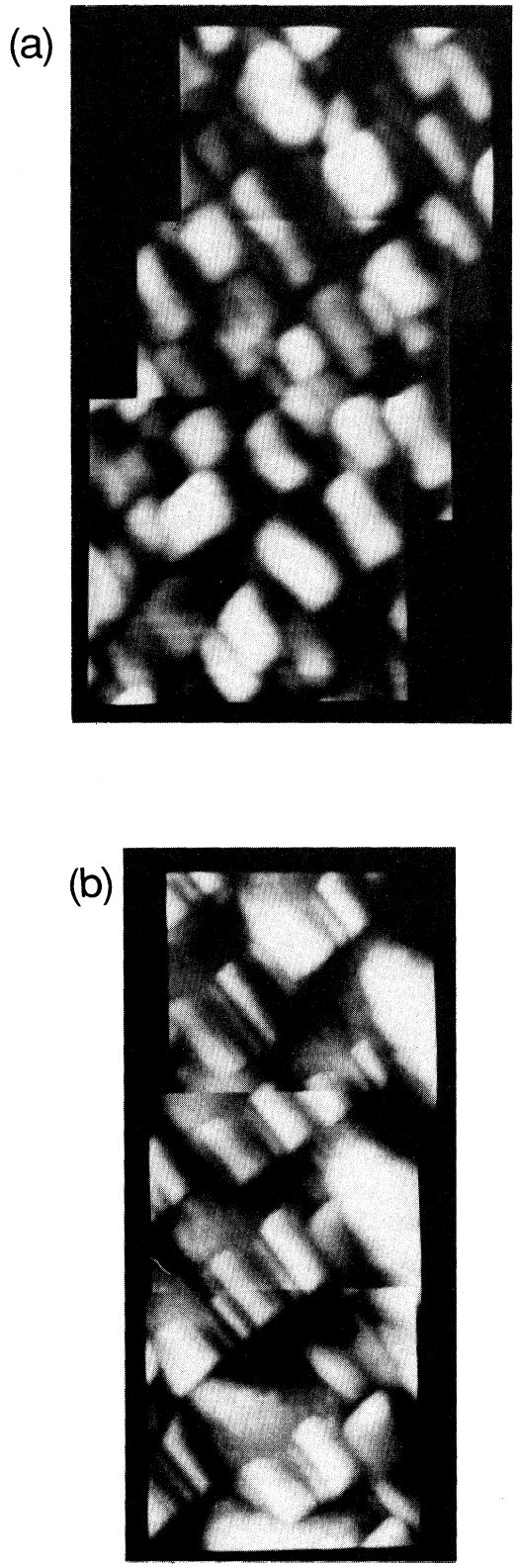

FIG. 3. Mosaic images of (a) 5-ML and (b) 10-ML Ag depositions showing the formation of nanocrystallites orientated along $[1\bar{1}0]$ and [001]. Each image used in the mosaic is $\sim 425 \times 425$ Å^2.

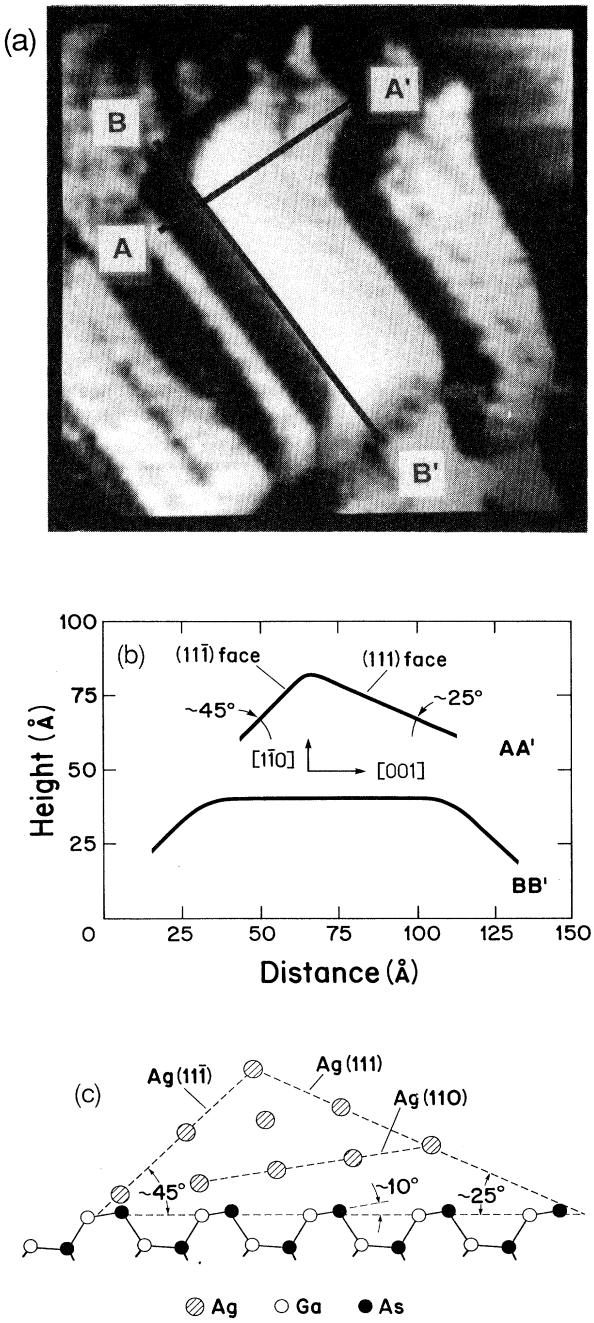

FIG. 4. (a) STM image of a typical Ag crystallite for 10-ML Ag on GaAs(110) acquired with a sample voltage of ~ 0.8 V showing facets, steps, and terraces. The length of $A-A'$ is ~ 70 Å. (b) Cross-sectional cuts along the crystallite in (a) along [001] $A-A'$ and $[1\bar{1}0]$ $B-B'$ directions showing the faceted faces of the crystal. The (111) and (11$\bar{1}$) faces of Ag have been labeled and the angles are given with respect to the substrate. (c) Schematic of the surface atomic geometry for the boundary layer between Ag and GaAs(110). The low-energy {111} facets are shown. The (110) plane of Ag is also identified, inclined 10° relative to the unrelaxed substrate (110) plane, but parallel to the partially unrelaxed surface. This establishes a structural arrangement such that four units of Ag correspond to three for GaAs.

might affect some detail of the cross section, the characteristic shapes of these big crystallites were independent of the tip used. Inclination angles of ~25° and ~45°, as labeled in Fig. 4(b) for $A-A'$, were measured from the cross section. These angles are in good agreement with those expected if facet orientations of (111) and (11$\bar{1}$) are assumed. The Ag(111) facet was clearly observed in our LEED investigation and in the LEED study of Bolmont *et al.*[24] The Ag(11$\bar{1}$) facet, however, was not decisively determined from LEED but was inferred from symmetry arguments.[24] The measurement of 45° inclination angle from the STM profile is a confirmation of their interpretation. Given that (111) and (11$\bar{1}$) of Ag are at 25° and 45° with respect to the substrate, the atomic plane of Ag parallel to the GaAs(110) can be determined to be (441). Bomont *et al.*[24] argued that the Ag periodicity in the [$\bar{1}\,\bar{1}$8] direction of the (441) plane is lattice matched within 2% of the GaAs(110), suggesting such a match could account for Ag(441) being in contact with GaAs(110). This lattice match is calculated by taking three times the GaAs periodicity in its [001] direction. No match can be found along [1$\bar{1}$0] between the substrate and overlayer. These facts suggest that the lattice match is not the driving force for the growth of Ag(441) on GaAs(110).

For an unreconstructed (110) surface of the diamond structure, there is a mirror symmetry about [1$\bar{1}$0]. Therefore, the overlayer structure grown on such a surface should preserve this symmetry, i.e., the (11$\bar{1}$) facet should be a mirror reflection of the (111) facet about [1$\bar{1}$0]. In this configuration, the (111) and (11$\bar{1}$) facets have an inclination angle of 35° with respect to GaAs(110), and the (110) face of the overlayer is parallel to GaAs(110). What we observe here for Ag/GaAs(110) is that Ag(111) and Ag(11$\bar{1}$) are exposed asymmetrically, establishing the Ag(110) surface at a 10° angle with respect to GaAs(110). It is interesting to note that the mirror symmetry on GaAs(110) is broken by having two types of atoms (Ga and As) on the surface and by the relaxation of the zig-zag chain. The relaxation of GaAs(110) causes the Ga—As bond to rotate around the [1$\bar{1}$0], resulting in a buckling angle of 27° (Ref. 19). The morphology of the relaxed surface therefore resembles a stepped surface. We believe that the observed asymmetry of the Ag crystallites is a consequence of the asymmetry of the GaAs(110) surface itself.

In Fig. 4(c) we show the model we propose based on the simple idea. The Ag(110) surface is parallel to the partially unrelaxed Ga—As bond that has a buckling angle of 10°. The change of the buckling angle from the clean substrate is expected due to the deposition of overlayer atoms. Photoemission experiments have shown[1,17] that the interaction between the Ag overlayer and the GaAs substrate is weak. As a consequence, the growth of the Ag crystallite is dictated by the interactions among Ag atoms. In our model, three times of the "step-height" (2.94 Å) is equal to the Ag atom spacing (2.89 Å) in the [110] direction. Hence, Ag atoms are able to stack on this "staircase" (the substrate) to build Ag crystallites. The asymmetry between the Ag(111) and the Ag(11$\bar{1}$) facets comes as a natural result of the formation of the Ag(110) plane on the "stepped" substrate. Without the persistence of this partial unrelaxation, one would expect symmetric Ag{111} facets at 35° with respect to the substrate.

The exposure of Ag{111} facets is consistent with {111} being the most energetically favorable orientation. Calculations of surface free energies and experiments on equilibrium crystal shape have shown the lowest energy facets are (111), (100), and (110) for Ag, in sequence of increasing free energy.[25] A cross-sectional view along the line BB' indicates facets at a 45° angle with respect to the substrate [Figs. 4(a) and 4(b)], which agrees well with {100} face formation. Ag{100} is the most favorable termination for the given crystallite structure. Our LEED measurements did not show clear patterns associated with {100} facets, presumably due to small facet size and large facet angle with respect to the incident electron beam. [A more elaborate LEED system should allow the identification of {100} and (11$\bar{1}$) facets.] Note that facets could also reflect kinetic effects since the experiments were performed at 300 K, but in this case one would expect to see them at lower coverage. The evidence indicates that the crystallites represent the surface-free-energy minimization of the Ag clusters, with thermodynamics dominating.

Insight into the 2D versus 3D character of the features that were formed during the early stages of growth can be gained by evaluating the relationship between the areas and volumes for isolated clusters. The results of such STM investigations after deposition of 0.25 ML of Ag at 300 K are shown in Fig. 5. The cluster measurements were made on ~100 clusters from an area of ~1500×1500 Å^2. Data such as these can be fit with a two-parameter power law, $V=kA^n$, where V is the cluster volume and A is the cluster area in contact with the substrate. With this relationship, n would equal 1 for 2D growth and 1.5 for equal growth rates in all three dimensions. The dashed line in Fig. 5 for $n=1.5$ clearly underestimates the volume-to-area ratio, and a linear behavior for 2D growth would deviate even more significantly.

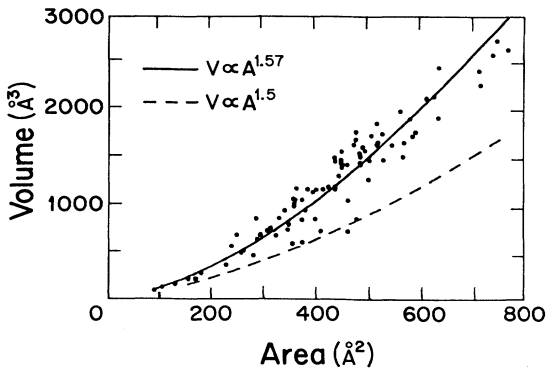

FIG. 5. Cluster volume (V) vs cluster area (A) calculated from STM images of 0.25-ML Ag on GaAs(110). The data have been fit with a two-parameter power law, $V\sim A^n$. The parameter n would be 1.0 for 2D growth but 1.5 for isotropic 3D growth. Our results suggest the best fit with $n=1.57$.

The best fit to the volume-area data was achieved with $n = 1.57$, indicating a three-dimensional growth. The only other system for which this analysis has been performed involved Fe growth on GaAs(110) at 300 K (Ref. 11), where the best fit was obtained with $n = 1.2$, suggesting that Fe was more 2D. We speculate that the disruption of the surface by Fe deposition and the subsequent incorporation into Fe clusters of Ga and As atoms influences the growth structures, but a broader data base would be needed to be more definite because surface and interface free energies would also play a role. In principle, the factor k could be used to infer whether growth favors a particular geometry (hemispherical, cuboid, etc), but such analysis does not seem justified.

The shape of the tunneling tip in general can affect the absolute value of volume measurement. In the case of Ag/GaAs(110), such an effect is expected to be minimal due to the large size of the clusters. In addition, the growth exponent describes the relation of the volume relative to the area and does not depend on the absolute measurement of volume and area. We therefore expect little tip effect on the value of the exponent.

During studies of Ag cluster growth for depositions of 0.05 ML or below, we have occasionally observed cluster movement. Figure 6 shows an example of this through sequential images of the same area. Comparison of Figs. 6(a) and 6(b) shows two clusters (labeled *A*) that have merged into one larger cluster. The original size of the clusters was ~100 and 250 atoms, respectively. This suggests that either the clusters are mobile or that the tip has interacted in such a way as to induce movement. Such movement is relatively rare, however, and when it occurs, there is generally a streak in the image. This would be consistent with a tip-induced effect. The movement of a Ag cluster as a whole by an STM tip further demonstrates the weak substrate-overlayer interaction and strong interaction among Ag atoms. We also note that areas exposed by cluster movement gave no indication of cluster-induced substrate disruption.

Finally, it is instructive to compare the growth structures observed here for Ag/GaAs(110) to those for other systems. Clusters have been shown to form at low coverage for Ag/GaAs(110), Cr/GaAs(110) (Ref. 10) and Fe/GaAs(110) (Ref. 11), but only Ag exhibits the evolution to faceted crystallites. For Cr/GaAs(110) and Fe/GaAs(110), the failure to do so is probably a consequence of substrate disruption. In particular, Ga and As atoms released from the substrate are incorporated in the cluster and they form complex bonding configurations.[1] In contrast, STM studies of Au/GaAs(110) (Ref. 12) have shown crystallite formation by 5-ML deposition and a preferential orientation relative to the substrate, even though Au deposition onto GaAs induces limited substrate disruption[1,16] While it is clear that the presence of Ga and As in the clusters must be taken into account, the tendency of these atoms to segregate to the surface and the effects of kinetic constraints make it difficult to predict the growth structures for disruptive overlayers. Ag growth represents the simplest case for modeling of growth because of the absence of the substrate disruption.

Comparison of the Ag/GaAs(110) results to those for Ag growth on Si(100)-2×1 (Refs. 26–28) and Si(111)-7×7 (Refs. 8, 29, and 30) suggests differences related to greater adatom-substrate interactions. For Ag/Si(100)-2×1, Samsavar *et al.*[26] showed a preferred chemisorption site and the formation of linear chains at low coverage. Their results suggested that adatom-substrate interactions were greater than adatom-adatom bonding. Continued growth on Si(100) led to cluster formation on a surface covered with linear chains. By 10 ML, crystallites covered the surface, and the STM images showed both (111) and (110) facets. Results for Ag/Si(111)-7×7 showed distinct reconstructed Ag overlayers and no indication of cluster growth, but the measurements were limited to the submonolayer-coverage regime.

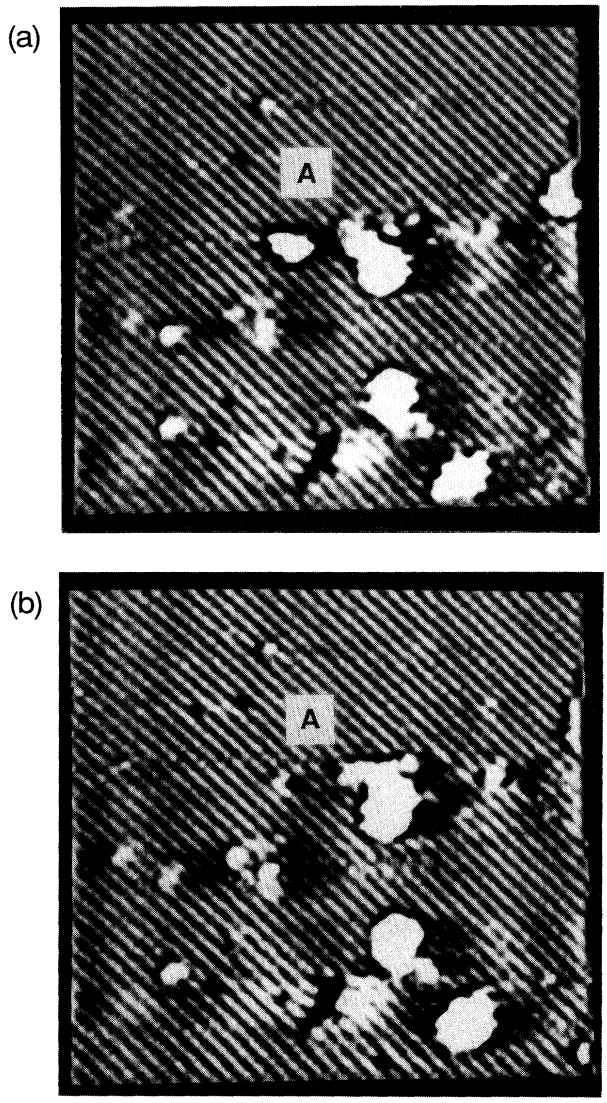

FIG. 6. STM images (a) and (b) for 0.05-ML Ag on GaAs(110) showing the interaction of the tip with cluster *A* and the subsequent movement of that cluster and its merging with another.

CONCLUSIONS

Perhaps the most interesting aspect of this study has been the observed tendency of the Ag clusters to evolve to faceted crystallites as the number of atoms in each cluster increases. Through quantitative analysis of the volume-area relation of clusters, we have determined Ag cluster growth to be three dimensional in nature. We have proposed a model that can account for the asymmetry of faceted Ag crystallites observed at high coverages. The orientation of the facets on the crystallites has been determined to be {111} and {100}, which are energetically favorable orientations for Ag metal. We do not believe kinetics would be a limitation for the energy minimization due to known large Ag mobility and the energy released by the formation of the crystallites. The evolution observed for Ag/GaAs(110) reflects a very fundamental property of this system—strong overlayer-overlayer interaction and weak substrate-overlayer interaction. Such strong bonding among Ag atoms and the lack of interaction with the substrate was explicitly demonstrated by moving a Ag cluster as a whole using the STM tip. The absence of a footprint on the substrate, where the cluster was located before movement by the STM tip, confirms the photoemission results that Ag is nondisruptive on GaAs(110).

ACKNOWLEDGMENTS

This work was supported by the National Science Foundation under Grant No. DMR-86-10837. We thank G. D. Waddill for useful discussions and Y.-S. Luo for developing the codes used to calculate the cluster volumes and areas. The cheerful assistance of the staff of Park Scientific Instruments was very much appreciated.

[1]J. H. Weaver, in *A New Era of Materials Science,* edited by J. R. Chelikowsky and A. Francosi (Springer-Verlag, Berlin, in press), Chap. 8, and references therein; J. W. Matthews, in *Epitaxial Growth,* edited by J. W. Matthews (Academic, New York, 1975).

[2]L. C. Feldman and J. W. Mayer, *Fundamentals of Surface Science and Thin Film Analysis* (North-Holland, New York, 1986).

[3]R. H. Williams, in *Physics and Chemistry of III-V Compound Semiconductor Interfaces,* edited by C. W. Wilmsen (Plenum, New York, 1985).

[4]R. Kern, G. LeLay, and J. J. Metois, in *Current Topics in Materials Science,* edited by E. Kaldis (North-Holland, Amsterdam, 1979), Vol. 3; E. Bauer and H. Poppa, Thin Films **12**, 167 (1972).

[5]See, for example, Y. Kuk and P. J. Silverman, Rev. Sci. Instrum. **60**, 165 (1989).

[6]See, *The Proceedings of the Second and Fourth International Conferences of Scanning Tunneling Microscopy* [J. Vac. Sci. Technol. A **6**, 401 (1988)]; **8**, 153 (1990).

[7]J. Nogami, A. A. Baski, and C. F. Quate, Phys. Rev. Lett. **65**, 1611 (1990); A. A. Baski, J. Nogami, and C. F. Quate, Phys. Rev. B **41**, 10247 (1990).

[8]R. J. Wilson and S. Chiang, Phys. Rev. Lett. **59**, 2329 (1987).

[9]Y.-W. Mo, B. S. Swartzentruber, R. Kariotis, M. B. Webb, and M. G. Lagally, Phys. Rev. Lett **63**, 2393 (1989).

[10]B. M. Trafas, D. M. Hill, P. J. Benning, G. D. Waddill, Y.-N. Yang, R. L. Siefert, and J. H. Weaver, Phys. Rev. B **43**, 7174 (1991) discussed STM and photoemission results for Cr/GaAs(110).

[11]J. A. Stroscio, P. N. First, R. A. Dragoset, L. J. Whitman, D. T. Pierce, and R. J. Celotta, J. Vac. Sci. Technol. A **8**, 284 (1990); R. A. Celotta, Mat. Res. Soc. Symp. Proc. **151**, 193 (1989).

[12]R. M. Feenstra, Phys. Rev. Lett. **63**, 1412 (1989); J. Vac. Sci. Technol. B **7**, 925 (1989).

[13]B. M. Trafas, D. M. Hill, R. L. Siefert, and J. H. Weaver, Phys. Rev. B **42**, 3231 (1990).

[14]P. Mårtensson and R. M. Feenstra, Phys. Rev. B **39**, 7744 (1989); R. M. Feenstra and P. Mårtensson, Phys. Rev. Lett. **61**, 447 (1988); A. B. McLean, R. M. Feenstra, A. Taleb-Ibrahimi, and R. Ludeke, Phys. Rev. B **39**, 12925 (1989).

[15]C. K. Shih, E. Kaxiras, R. M. Feenstra, and K. C. Pandey, Phys. Rev. B **40**, 10044 (1989).

[16]F. Xu, Y. Shapira, D. M. Hill, and J. H. Weaver, Phys. Rev. B **35**, 7417 (1987); M. Grioni, J. J. Joyce, and J. H. Weaver, J. Vac. Sci. Technol. A **4**, 964 (1986).

[17]See, for example, G. D. Waddill, C. M. Aldao, I. M. Vitomirov, S. G. Anderson, C. Capasso, and J. H. Weaver, J. Vac. Sci. Technol. B **7**, 950 (1989), and references therein.

[18]Park Scientific Instruments Model No. STM-SU2, Mountain View, CA.

[19]R. M. Feenstra, J. A. Stroscio, J. Tersoff, and A. P. Fein, Phys. Rev. Lett. **58**, 1192 (1987).

[20]L. J. Whitman, J. A. Stroscio, R. A. Dragoset, and R. J. Celotta, Phys. Rev. B **42**, 7280 (1990).

[21]A. Zur, T. C. McGill, and D. L. Smith, Phys. Rev. B **28**, 2060 (1983).

[22]Y.-N. Yang, B. M. Trafas, R. L. Siefert, and J. H. Weaver, Phys. Rev. B (to be published). See also R. Moller, R. Coenen, B. Koslawski, and M. Rauscher, Surf. Sci. **217**, 289 (1989).

[23]Preferred diffusion has been predicted to occur along $[1\bar{1}0]$ for Al on GaAs(110), as discussed by J. Ihm and J. D. Joannopoulos, Phys. Rev. B **26**, 4429 (1982).

[24]D. Bolmont, P. Chen, F. Proix, and C. A. Sebenne, J. Phys. C. **15**, 3639 (1982).

[25]B. E. Sundquist, Acta Metall. **12**, 67 (1964).

[26]A. Samsavar, E. S. Hirschorn, F. M. Leibsle, and T.-C. Chiang, Phys. Rev. Lett. **63**, 2830 (1989).

[27]A. Brodde, D. Badt, St. Tosch, and H. Neddermeyer, J. Vac. Sci. Technol. A **8**, 251 (1990).

[28]T. Hashizume, R. J. Hamers, J. E. Demuth, K. Market, and T. Sakurai, J. Vac. Sci. Technol. A **8**, 249 (1990).

[29]St. Tosch and H. Neddermeyer, Phys. Rev. Lett. **61**, 349 (1988).

[30]E. J. van Loenen, J. E. Demuth, R. M. Tromp, and R. J. Hamers, Phys. Rev. Lett. **58**, 373 (1987).

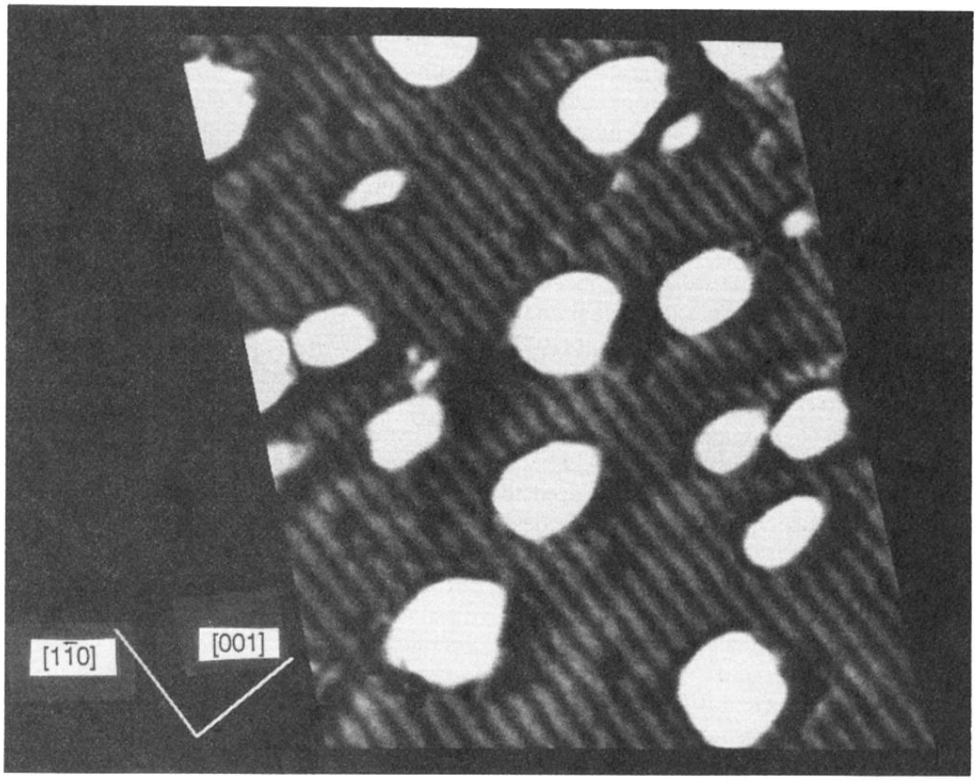

FIG. 1. STM image of GaAs(110) following evaporation of 0.25 ML of Ag at 300 K for an area of 120×120 Å^2. The image was acquired with a sample voltage of -1.9 V and corresponds to imaging As atoms. Dark depressions represent surface defects, whereas the bright areas reflect 3D clusters of Ag. The typical volume of these clusters is ~150–2500 Å^3.

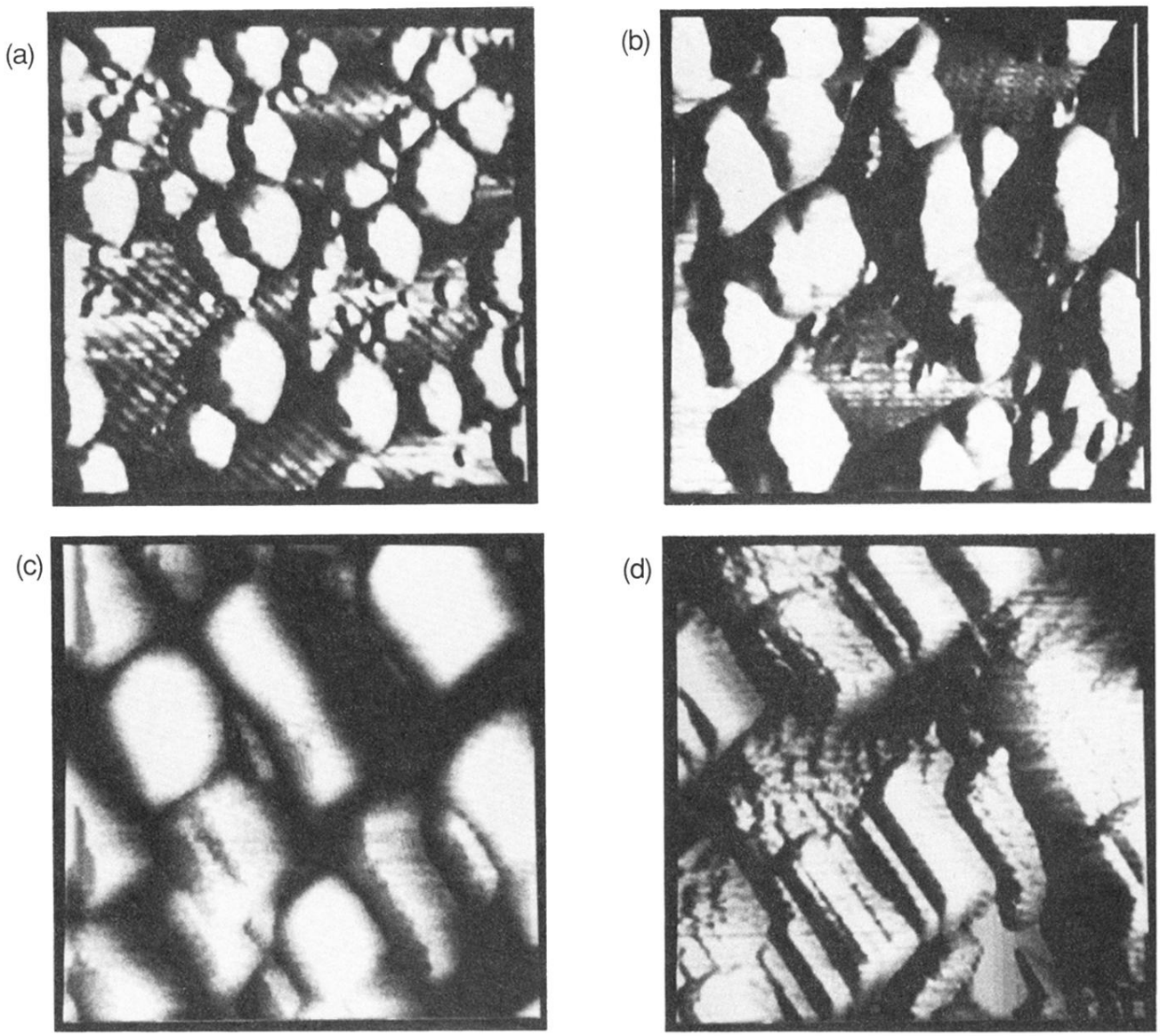

FIG. 2. (a)–(d) STM images of Ag overlayer growth by atom deposition onto GaAs(110) at 300 K for coverages of (a) 0.5, (b) 1.5, (c) 5, and (d) 10 ML of Ag on GaAs(110). The areas imaged are 220×220, 320×320, 425×425, and 425×425 Å^2, respectively. Images (a) and (b) were obtained with a sample bias of -2.5 V and a tunneling current of 0.1 nA. Images (c) and (d) were obtained with -0.8 V and 1 nA to enhance the contrast of the metal surface. The gray scale in these images is computed according to a surface directional derivative, corresponding to illumination from a point in the upper-right corner of each image. Ag clustering is apparent in (a) and (b). Faceting and the transition to crystallites is evident in (c) and (d) where the long dimension is along $[1\bar{1}0]$ and the short dimension is along [001].

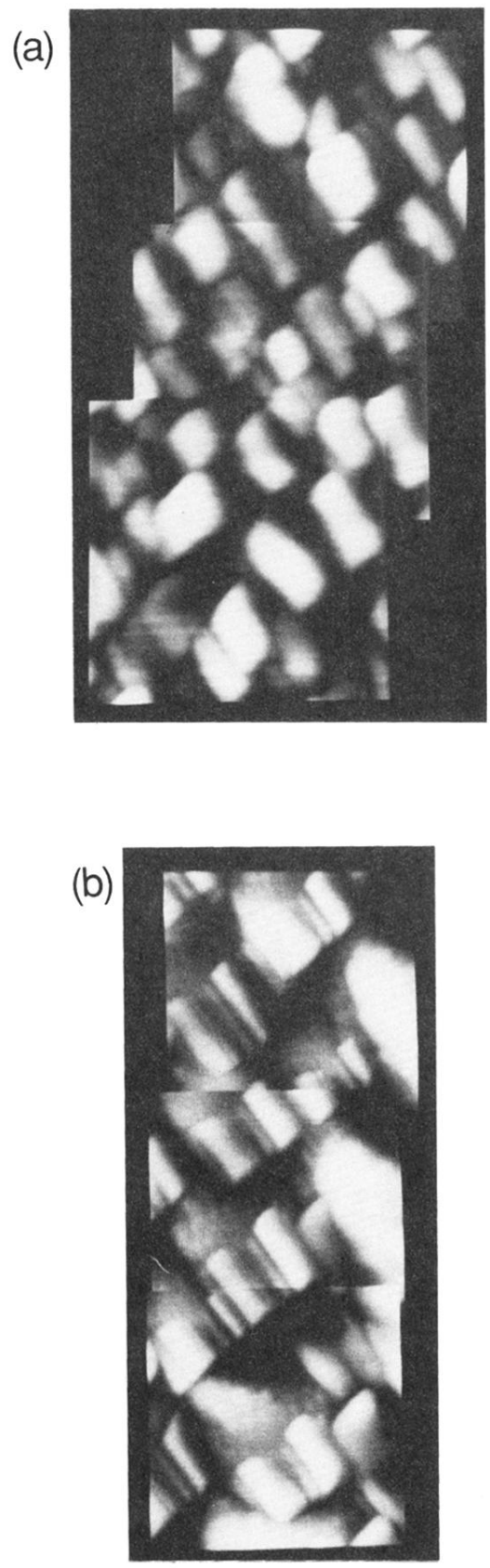

FIG. 3. Mosaic images of (a) 5-ML and (b) 10-ML Ag depositions showing the formation of nanocrystallites orientated along $[1\bar{1}0]$ and [001]. Each image used in the mosaic is $\sim 425 \times 425$ Å^2.

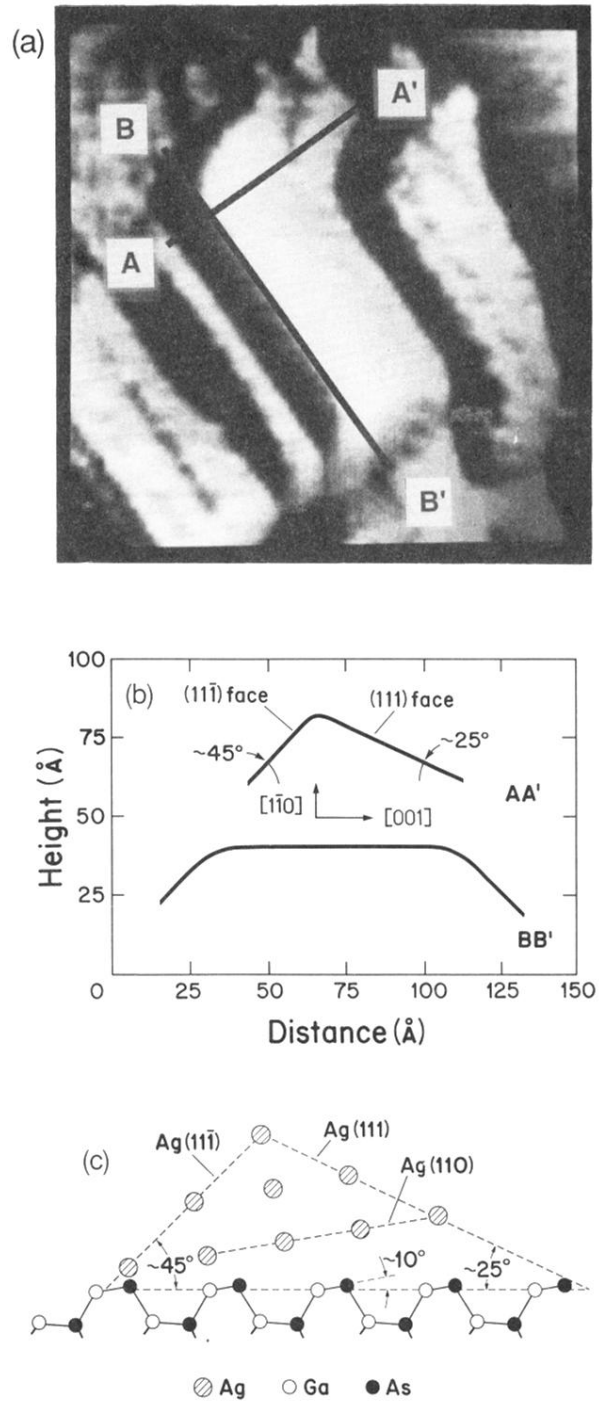

FIG. 4. (a) STM image of a typical Ag crystallite for 10-ML Ag on GaAs(110) acquired with a sample voltage of ~ 0.8 V showing facets, steps, and terraces. The length of $A-A'$ is ~ 70 Å. (b) Cross-sectional cuts along the crystallite in (a) along [001] $A-A'$ and [1$\bar{1}$0] $B-B'$ directions showing the faceted faces of the crystal. The (111) and (11$\bar{1}$) faces of Ag have been labeled and the angles are given with respect to the substrate. (c) Schematic of the surface atomic geometry for the boundary layer between Ag and GaAs(110). The low-energy {111} facets are shown. The (110) plane of Ag is also identified, inclined 10° relative to the unrelaxed substrate (110) plane, but parallel to the partially unrelaxed surface. This establishes a structural arrangement such that four units of Ag correspond to three for GaAs.

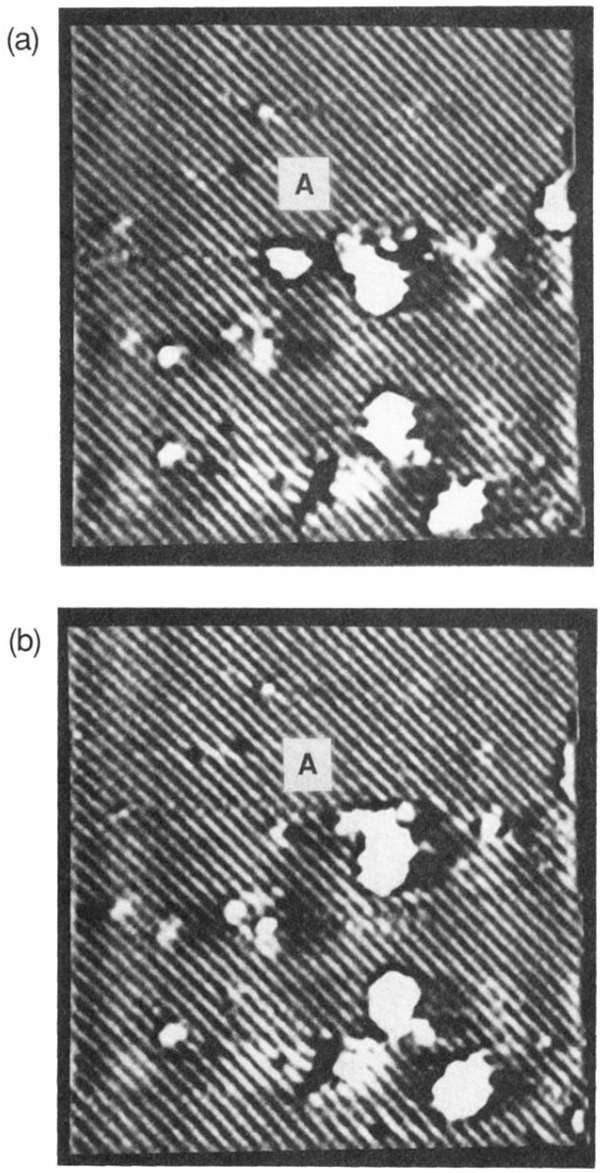

FIG. 6. STM images (a) and (b) for 0.05-ML Ag on GaAs(110) showing the interaction of the tip with cluster *A* and the subsequent movement of that cluster and its merging with another.